

SCATTERED NUCLEAR CONTINUUM AND BROAD H α IN CYGNUS A

P. M. OGLE AND M. H. COHEN

Mail Stop 105-24, California Institute of Technology, Pasadena, CA 91125; pmo@astro.caltech.edu

J. S. MILLER AND H. D. TRAN¹

UCO/Lick Observatory, University of California, Santa Cruz, CA 95064

R. A. E. FOSBURY²

Space Telescope–European Coordinating Facility, Karl-Schwarzschild Str. 2, D-85748, Garching bei Munchen, Germany

AND

R. W. GOODRICH

W. M. Keck Observatory, 65-1120 Mamalahoa Highway, Kamuela, HI 96743

Received 1997 January 28; accepted 1997 March 20

ABSTRACT

We have discovered scattered broad Balmer emission lines in the spectrum of Cygnus A, using the Keck II Telescope. Broad H α appears in polarized flux from components on either side of the nucleus and, to a lesser extent, in the nucleus. The full-width at half-maximum of broad H α is 26,000 km s⁻¹, comparable to the widest emission lines seen in broad-line radio galaxies. Scattered active galactic nucleus light provides a significant contribution to the total flux at 3800 Å (rest) of the western component, where the polarization rises to 16%. The spatially integrated flux of Cygnus A at 5500 Å can be decomposed into an elliptical galaxy fraction ($F_g = 0.70$), a highly polarized blue component (FC1 = 0.15), a less polarized red component (FC = 0.09), and a contribution from the nebular continuum (0.06). Imaging polarimetry shows a double fan of polarization vectors with circular symmetry that corresponds to the ionization cone seen in *Hubble Space Telescope* images. Our results are consistent with scattering of light from a hidden quasar of modest luminosity by an extended, dusty narrow-line region.

Subject headings: galaxies: active — galaxies: individual (Cygnus A)

1. INTRODUCTION

In recent years there has been considerable interest in the unification of active galaxies. In part this was stimulated by the discovery (Antonucci & Miller 1985) that the nucleus of the Seyfert 2 galaxy NGC 1068 contains a broad-line region (BLR) obscured from direct view, but visible in scattered light. This result gives support to the hypothesis that Seyfert type 1 and type 2 galaxies are the same kind of object seen from different aspects. Barthel (1989) extends this picture to quasars and radio galaxies, proposing that narrow-line radio galaxies (NLRG) of Fanaroff-Riley type 2 contain quasars that are obscured from our viewing direction. He finds that this hypothesis is consistent with the relative numbers of quasars and appropriate radio galaxies in the 3C Catalogue if the quasar is visible from any direction within a cone of half-opening angle about 45°. Beyond that cone the optical continuum source and BLR would be obscured from direct view.

Attempts to detect hidden BLRs in radio galaxies have had some success (e.g., 3C 234, Antonucci 1984 and Tran, Cohen, & Goodrich 1995; 3C 321, Young et al. 1996). High polarization perpendicular to the radio axis and broad Mg II suggest the presence of hidden quasars in high redshift radio galaxies as well (e.g., di Serego Alighieri, Cimatti, & Fosbury 1994; Cimatti et al. 1996). According to the Barthel hypothesis, the prototypical NLRG containing the exceptionally strong radio

source Cygnus A (3C 405) should harbor an obscured quasar. Djorgovski et al. (1991) present evidence from infrared observations that Cygnus A does contain a luminous quasar. Imaging polarimetry by Tadhunter, Scarrott, & Rolph (1990) suggests that there is an extended region that scatters light from a hidden nucleus. Broad Mg II is detected by Antonucci, Hurt, & Kinney (1994, hereafter AHK) in the ultraviolet. In spite of considerable effort (e.g., Goodrich & Miller 1989; Jackson & Tadhunter 1993), previous attempts to detect broad lines in polarized flux have been unsuccessful. In this Letter we present spectropolarimetry from the Keck II Telescope that shows broad lines seen in scattered light originating from an obscured nuclear region. Cygnus A does indeed contain an obscured active galactic nucleus (AGN) with broad permitted lines, giving additional weight to the radio galaxy–quasar unification hypothesis. Section 2 summarizes the observations, and § 3 and § 4 present the results and their implications, respectively.

2. OBSERVATIONS AND REDUCTIONS

We observed Cygnus A with the Low-Resolution Imaging Spectrograph polarimeter on 1996 October 4 and 5 with the Keck II Telescope (four nights after scientific commissioning). The first night of observations included 1 hr of *B*-band imaging polarimetry. On the second night 2.2 hr of spectropolarimetry were taken with a 300 line mm⁻¹ grating blazed at 5000 Å. A 1" slit was placed at a position angle of 101° to include the highly polarized western knot, the eastern knot, and the nuclear knot. This slit location (indicated in Fig. 1) is nearly

¹ Current address: Institute of Geophysics and Planetary Physics, Lawrence Livermore National Laboratory L-413, Livermore, CA 94550.

² Affiliated to the Astrophysics Division, Space Science Department, European Space Agency.

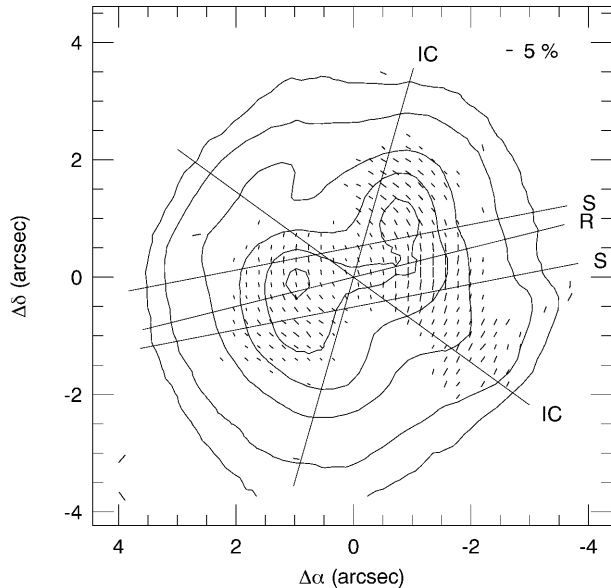


FIG. 1.—*B*-band imaging polarimetry of Cygnus A. Polarization vectors with $\text{SNR} \geq 2.5$ are plotted for each $0.212''$ pixel over the flux contours (20%, 25%, 41%, 60%, 81%, 97%). The centrosymmetric pattern of vectors indicates scattering of light from a hidden central source. This scattered light cone matches the 55° half-angle ionization cone (IC) seen in *HST* images. The radio axis (R) and slit used for spectropolarimetry (S) are also indicated.

along the radio axis, which is at 104° on kiloparsec scales. The data are reduced using standard procedures (Miller, Robinson, & Goodrich 1988; Cohen et al. 1997). Prior to calculating the Stokes parameters (Q , U), the flux was binned by 4 pixels to improve the signal-to-noise ratio (SNR), which drops below 3.0 for Q at 7200 \AA (rest). The fractional polarization (P) is estimated by rotating the Stokes parameters. The spectroscopy is calibrated using BD +28°4211 as a flux standard and HD 155528 as a polarimetric standard. On the first night the telescope would not come to a sharp focus, so stellar images are elongated northwest-southeast with a seeing ellipse of $1''.0 \times 0''.8$. The seeing in the spectra is $0''.6$ – $1''.0$ along the slit. There were patchy cirrus clouds on the first night and photometric conditions on the second night.

The Galactic interstellar reddening is determined from a $m_V = 19.6$ star $10''$ east of Cygnus A, which was also on the slit. We classify this star as an F9V main sequence star using standard templates (Jacoby, Hunter, & Christian 1984) and derive a reddening index of $E(B - V) = 0.495 \pm 0.015$ from the Cardelli, Clayton, & Mathis (1989) curve. The corresponding extinction is $A_V = 1.5$ mag. After correcting for extinction, the spectroscopic distance to the star is 6.0 kpc (610 pc above the Galactic plane), making it a good probe of Galactic reddening. Our value for $E(B - V)$ is significantly greater than the average (0.36) given by Spinrad & Stauffer (1982) for galaxies within $4'$ of Cygnus A. However, it is consistent with reddening estimates obtained by Tadhunter (1996) from the Cygnus A $\text{H}\alpha/\text{H}\beta$ line ratio.

We correct our spectra for Galactic reddening, then subtract a scaled template derived from the elliptical galaxy NGC 821. The best fit for the galaxy fraction at 5500 \AA is $F_g = 70\% \pm 2\%$, obtained using the procedure of Tran (1995a). Interstellar Na I D absorption in our Galaxy shows an equivalent width in the presubtracted spectrum of $2.0 \pm 0.1 \text{ \AA}$, broadly consistent with the Galactic reddening (Bica & Alloin 1986). We do not

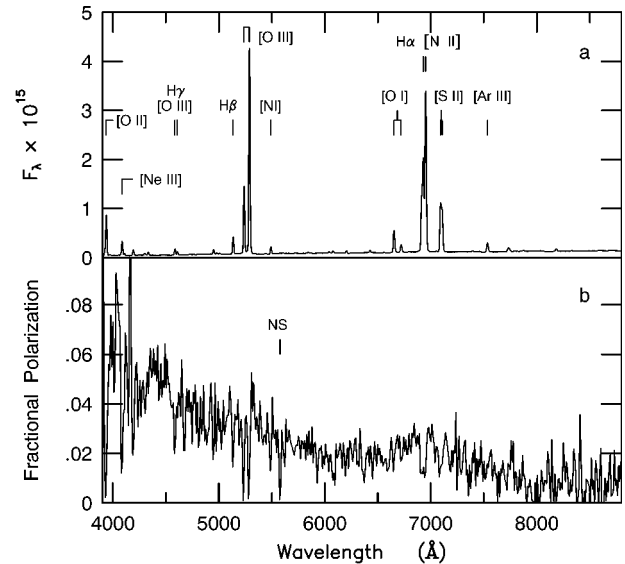


FIG. 2.—Spectropolarimetry of Cygnus A. The spectra are integrated along $7''.6$ of the slit, including the nucleus, eastern lobe, and western lobe (see Fig. 1). (a) Total flux. (b) Observed fractional polarization. P rises from $\sim 1\%$ in the red to 6% in the blue. P drops in the narrow emission lines and rises at the location of broad $\text{H}\alpha$. The noise feature at 5577 \AA is due to night sky (NS) line emission.

correct the data for interstellar polarization, which is expected to be small in the *B* band (Jackson & Tadhunter 1993). A correction of 0.5% would rotate most of the Cygnus A polarization vectors by about 3° .

3. RESULTS

Figure 1 shows the imaging polarimetry of Cygnus A. This *B*-band image reveals two fans of scattered polarized light, with the symmetry of the vectors clearly indicating a central source. After considering the effects of seeing, the scattered light cone matches the ionization cone with 55° half-opening angle seen in the *Hubble Space Telescope* (*HST*) image of Jackson et al. (1996, hereafter JTS). The outline of this cone is shown in Figure 1, with the apex chosen to be consistent ($\pm 0''.5$) with the polarization pattern and the *HST* image. The *B*-band polarization peaks at $10.8\% \pm 0.8\%$ at the position of the western knot in the *HST* image by JTS. The intrinsic polarization of this knot must be even greater after correcting for unpolarized galaxy light.

We present the spectropolarimetry in Figures 2 and 3. Figure 2 shows the flux and polarization spectra integrated along $7''.6$ of the slit. P rises from $\sim 1\%$ in the red to 6% in the blue, and there is a broad rise in P centered on $\text{H}\alpha$. P drops in the narrow lines, which have $P = 1.3\%$ at P.A. = 32° . In polarized flux (Fig. 3), the narrow lines are redshifted 110 – 230 km s^{-1} , with the redshift greatest in the high ionization lines in the eastern cone. The polarized narrow lines are not broadened, suggesting that their polarization is at least partly due to dust scattering in an outflowing wind, analogous to the phenomenon observed in planetary nebulae (Walsh & Clegg 1994). However, transmission through dust in our Galaxy and Cygnus A may affect the narrow line polarization.

Separate spectra of the eastern, western, and nuclear components are extracted using widths of $1''.3$, $0''.8$, and $1''.1$, respectively. The galaxy fractions at 5500 \AA in the eastern and western components are $64\% \pm 3\%$ and $62\% \pm 3\%$, respectively. Broad lines are visible in the dereddened polarized flux

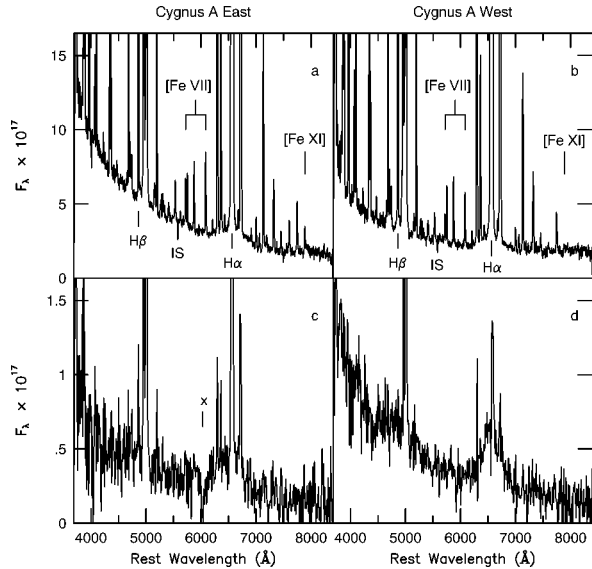


FIG. 3.—Separate extractions of the eastern and western components of Cygnus A. (a, b) Galaxy subtracted flux. (c, d) Polarized flux (bin = 4). Scattered blue continuum and broad H α emission are most prominent in the western component. There is an extremely blue contribution to the total flux in the eastern component which does not show up in polarized flux. The high ionization iron lines are relatively stronger by about a factor of 2 in the eastern component. Galactic interstellar Na I D absorption (IS) is also apparent. In panel c, the dip at 6000 Å is due to a cosmic-ray event.

spectra (Figs. 3c and 3d) and in the dereddened, galaxy subtracted total flux (Figs. 3a and 3b) of the eastern and western components. Broad lines are also present in the nuclear component at a lower level. Broad H α has a Galactic extinction-corrected total flux of 5×10^{-15} ergs cm $^{-2}$ s $^{-1}$ and a full-width at half-maximum (FWHM) of $\sim 26,000$ km s $^{-1}$ in both the eastern and western components. This is extremely broad, similar to the broadest radio galaxy emission lines (e.g., 3C 332, Eracleous & Halpern 1994). Broad H β is also visible in the polarized flux of the western component (Fig. 3d). The polarization of the western component rises to 16% at 3800 Å, suggesting that a large fraction of the continuum is scattered light.

Our high-quality spectra of Cygnus A display emission lines with a wide range of ionization. Identifications are made of [Fe III], [Fe V], [Fe VI], [Fe VII], and [Fe XI], but the feature at 5305 Å can probably be attributed to [Ca V] rather than [Fe XIV], and there is only a marginal detection of [Fe X] $\lambda 6375$. The most significant changes in relative line intensity with position along the slit are for [Fe VII] and [Fe XI], which are stronger to the east of the nucleus (Fig. 3).

4. DISCUSSION

4.1. Hidden AGN

The symmetric pattern of polarization vectors in the imaging polarimetry strongly suggests that we are seeing light from the central AGN scattered by material inside a bi-cone of illumination defined by an obscuring torus. While Tadhunter et al. (1990) found $P = 1\% - 2\%$ in V band, perpendicular to the radio axis, and concluded that Cygnus A is a “giant reflection nebula,” the much higher degree of polarization (11%) and greatly improved resolution in our B -band map make a stronger case for this interpretation. VLBI observations of the jet/counterjet flux ratio (Carilli & Barthel 1996 and references therein) constrain the inclination of the jet to

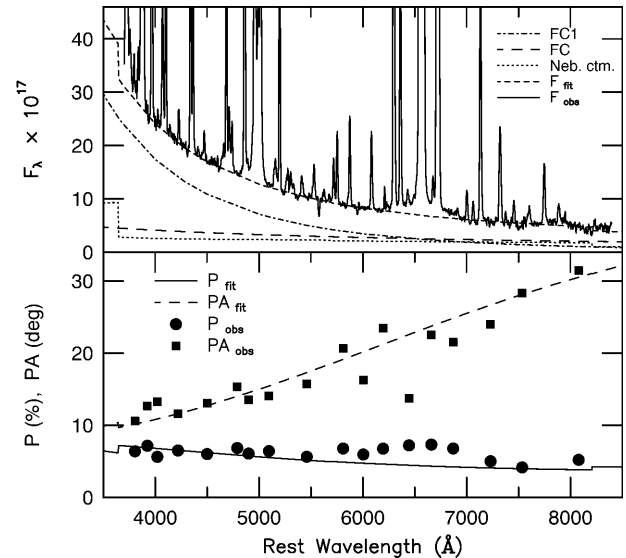


FIG. 4.—Continuum fits to the spatially integrated spectropolarimetric data. Observations are corrected for unpolarized host galactic starlight. P and P.A. are calculated in wavelength bins which avoid strong emission lines and are therefore, with the exception of several points near H α , dominated by continuum flux. The nebular continuum has been included with the same polarization properties as the narrow emission lines. The combination of two additional continua having power-law spectra with different (wavelength independent) P and P.A. is able to well represent the observed continuum flux and polarization properties. FC1 has $F_{\nu} \propto \nu^{\alpha}$ with $\alpha = +2$, $F_{6563} = 2.4 \times 10^{-17}$ ergs cm $^{-2}$ s $^{-1}$ Å $^{-1}$, $P = 9\%$ and P.A. = 6°. FC has $\alpha = -1$, $F_{6563} = 2.5 \times 10^{-17}$ ergs cm $^{-2}$ s $^{-1}$ Å $^{-1}$, $P = 6\%$ and P.A. = 48°. Fitting uncertainties in P and P.A. are approximately 1% and 3°, respectively.

$50^{\circ} < i < 85^{\circ}$ and show that the western side is in front of the eastern side. We obtain an independent estimate of the inclination by assuming that the radio and ionization cone axes coincide and that the line of sight must be outside this cone for the nucleus to remain hidden. In this case, the cone half-angle lies in the range $46^{\circ} < \theta < 55^{\circ}$, consistent with the Barthel (1989) hypothesis, and the inclination lies in the range $46^{\circ} < i < 90^{\circ}$, which matches the VLBI constraints. Forward scattering by dust should increase the contribution of scattered light in the front cone relative to the unpolarized components, thereby raising the fractional polarization in the west.

Seen in polarized flux (Fig. 3), Cygnus A resembles a broad-line AGN. The observed ratio of broad H α to broad Mg II (see AHK) in the eastern component is 2.0, which becomes 0.38 after correcting for Galactic reddening. Typical quasar ratios are 2–3 (Francis et al. 1991; Osterbrock 1989), suggesting that the broad lines are scattered by dust with efficiency following a $\sim \lambda^{-2}$ law. However, the H α FWHM (in km s $^{-1}$) is 3.5 times that measured for Mg II by AHK, making the comparison of these lines questionable. The broad lines are reflected from extended material at ~ 1 kpc, making variability an unlikely explanation of previous H α nondetections. Instead, the unusually large width of H α and large galaxy fraction probably led to previous underestimates of upper limits to the H α flux.

4.2. Spectral Fitting

The variation of P and P.A. across the spectrum of Cygnus A can be characterized with three differently polarized continuum components, each with a wavelength independent P and P.A. (Fig. 4). There is a nebular continuum computed from the observed (Galactic extinction corrected) H β narrow

line flux of 2.2×10^{-14} ergs cm^{-2} s^{-1} . This is then reddened by $E(B - V) = 0.69$ and given the same P and P.A. as the narrow emission lines. The remaining flux is attributed to a scattered continuum, FC1, polarized similarly to broad $\text{H}\alpha$ and another featureless continuum (FC), which is redder and has lower polarization at a different P.A. Note that FC is different from the FC2 component invoked to explain the polarization behavior of other AGN (Tran 1995b; Tran et al. 1995) because it is polarized. Figure 4 shows the result of the continuum component fitting to the spatially integrated spectropolarimetric data. The blueness and high polarization of FC1 is consistent with dust scattering. The redder FC component could include locally scattered and/or dichroically absorbed radiation from hot young stars associated with the knotty structures seen in the *HST* image (JTS) and analogous to the polarized radiation seen in the dust band in Centaurus A (Scarrott et al. 1996).

The colors of the total and polarized flux vary dramatically between the eastern and western components (Fig. 3). The polarized flux is bluer in the western component than in the eastern component, but the opposite is true of the total flux spectra. The spectral indices (4000–8000 Å, rest) of the total flux from the eastern and western components after dereddening and galaxy subtraction are $\alpha = 0.4$ and $\alpha = -0.4$, respectively, but a single power law ($f \sim \nu^\alpha$) is not a good fit. Models of the spatially separated components will be given in a later paper, but a fit to the full data set shows that FC1 dominates in the blue and in the western lobe, while the other FC component dominates in the red and in the eastern lobe. Furthermore, there must be significant internal reddening of both FC1 and FC in the western lobe but little in the east.

4.3. Luminosity of the Hidden AGN

Cygnus A contains a broad-line AGN, but is it luminous enough to be classified as a quasar? We estimate the absolute magnitude (M) of the central source from the highly polarized flux scattered by the western knot. For optically thin scattering,

$$M = M_{\text{PF}} - 2.5 \log \left(\frac{1}{q\tau P} \right) - A,$$

where M_{PF} is the absolute magnitude of the polarized flux, q is the central source covering fraction, τ is the scattering optical depth, P is the intrinsic polarization of the scattered light, and A is the extinction. We measure $M_{\text{PF}} = -14.4$ (rest B band) for the western component, assuming a Hubble constant of 73 km

s^{-1} Mpc^{-1} and correcting for Galactic extinction. The polarization of the scattered light is at least as great as the measured value in the rest B band, $P = 11\%$. The source covering fraction of the western knot is estimated to be $q = 0.86\%$ from the JTS image. Using these values we find $M_B = -22.0 + 2.5 \log \tau - A_B$.

An optical depth $\tau \leq 0.4$ or extinction $A_B \geq 1.0$ would elevate Cygnus A to the status of a quasar ($M_B \leq -23$), but it would still be weak compared with other hidden quasars such as 3C 234 and 3C 265 (Tran et al. 1995; Cohen et al. 1996). This agrees with Tadhunter (1996), who concludes that Cygnus A contains a “feeble” hidden AGN. In addition, the far-infrared luminosity of Cygnus A is extremely weak for its radio lobe power (see, e.g., Barthel & Arnaud 1996). So while Cygnus A may qualify as a quasar, it is probably a modest one.

5. CONCLUSIONS

Cygnus A, the prototypical narrow-line radio galaxy and by far the most powerful radio source out to a redshift $z = 1$, contains a hidden broad-line AGN. The double fan of centrosymmetric polarization vectors seen in imaging polarimetry clearly indicates a scattering origin and corresponds to the ionization cone seen in *HST* images. AGN light is reflected from material that has a direct view of the central source. Spectropolarimetry reveals broad $\text{H}\alpha$ and $\text{H}\beta$ emission lines and a blue continuum (FC1) seen in scattered light in the eastern and western fans. This confirms the radio galaxy–quasar unification by orientation hypothesis. The ratio of broad lines, blueness of FC1, and narrow line polarization are all consistent with scattering by dust. We also find a second polarized continuum (FC), which is redder than FC1 and has a different P.A. The luminosity of the central source is still uncertain but appears to be weak for its radio power.

We thank the Keck Observatory staff who made our observations with the newly commissioned Keck II Telescope possible. We also thank R. Blandford, S. Djorgovski, and J. Walsh for helpful discussions. H. D. T. thanks the ST-ECF/European Southern Observatory for its hospitality during his visit. The W. M. Keck Observatory is operated as a scientific partnership between the California Institute of Technology and the University of California; it was made possible by the generous financial support of the W. M. Keck Foundation. This research has made use of the NASA/IPAC Extragalactic Database (NED).

REFERENCES

- Antonucci, R. R. J. 1984, *ApJ*, 278, 499
 Antonucci, R., Hurt, T., & Kinney, A. 1994, *Nature*, 371, 313 (AHK)
 Antonucci, R. R. J., & Miller, J. S. 1985, *ApJ*, 297, 621
 Barthel, P. D. 1989, *ApJ*, 336, 606
 Barthel, P. D., & Arnaud, K. A. 1996, *MNRAS*, 283, L45
 Bica, E., & Alloin, D. 1986, *A&A*, 166, 83
 Cardelli, J. A., Clayton, G. C., & Mathis, J. S. 1989, *ApJ*, 345, 245
 Carilli, C. L., & Barthel, P. D. 1996, *A&A Rev.*, 7, 1
 Cimatti, A., Dey, A., Van Breugel, W., Antonucci, R., & Spinrad, H. 1996, *ApJ*, 465, 145
 Cohen, M. H., Tran, H. D., Ogle, P. M., & Goodrich, R. W. 1996, in *IAU Symp. 175, Extragalactic Radio Sources*, ed. R. Ekers (Dordrecht: Kluwer), 223
 Cohen, M. H., Vermeulen, R. C., Ogle, P. M., Tran, H. D., & Goodrich, R. W. 1997, *ApJ*, in press
 di Serego Alighieri, S., Cimatti, A., & Fosbury, R. A. E. 1994, *ApJ*, 431, 123
 Djorgovski, S., Weir, N., Matthews, K., & Graham, J. R. 1991, *ApJ*, 372, L67
 Eracleous, M., & Halpern, J. P. 1994, *ApJS*, 90, 1
 Francis, P. J., Hewett, P. C., Foltz, C. B., Chaffee, F. H., Weymann, R. J., & Morris, S. L. 1991, *ApJ*, 373, 465
 Goodrich, R. W., & Miller, J. S. 1989, *ApJ*, 346, L21
 Jackson, N., & Tadhunter, C. N. 1993, *A&A*, 272, 105
 Jackson, N., Tadhunter, C., Sparks, W. B., Miley, G. K., & Macchetto, F. 1996, *A&A*, 307, L29 (JTS)
 Jacoby, G. H., Hunter, D. A., & Christian, C. A. 1984, *ApJS*, 56, 257
 Miller, J. S., Robinson, L. B., & Goodrich, R. W. 1988, in *Instrumentation of Ground-Based Astronomy*, ed. L. B. Robinson (New York: Springer), 157
 Osterbrock, D. E. 1989, *Astrophysics of Gaseous Nebulae and Active Galactic Nuclei* (Mill Valley: University Science Books)
 Scarrott, S. M., Foley, N. B., Gledhill, T. M., & Wolstencroft, R. D. 1996, *MNRAS*, 282, 252
 Spinrad, H., & Stauffer, J. R. 1982, *MNRAS*, 200, 153
 Tadhunter, C. 1996, in *Cygnus A—Study of a Radio Galaxy*, ed. C. L. Carilli & D. E. Harris (Cambridge: Cambridge Univ. Press), 33
 Tadhunter, C. N., Scarrott, S. M., & Rolph, C. D. 1990, *MNRAS*, 236, 163
 Tran, H. D. 1995a, *ApJ*, 440, 565
 ———, 1995b, *ApJ*, 440, 597
 Tran, H. D., Cohen, M. H., & Goodrich, R. W. 1995, *AJ*, 110, 2597
 Walsh, J. R., & Clegg, R. E. S. 1994, *MNRAS*, 268, L41
 Young, S., Hough, J. H., Efstathiou, A., Wills, B. J., Axon, D. J., Bailey, J. A., & Ward, M. J. 1996, *MNRAS*, 279, L72